

NUREG/CR-5433
SAND89-1951

Validation of Models of Gas Holdup in the CORCON Code

Prepared by J. E. Brockmann, F. E. Arellano, D. A. Lucero

Sandia National Laboratories

Prepared for
U.S. Nuclear Regulatory Commission

9001100257 891231
PDR NUREG
CR-5433 R PDR

AVAILABILITY NOTICE

Availability of Reference Materials Cited in NRC Publications

Most documents cited in NRC publications will be available from one of the following sources:

1. The NRC Public Document Room, 2120 L Street, NW, Lower Level, Washington, DC 20555
2. The Superintendent of Documents, U.S. Government Printing Office, P.O. Box 37082, Washington, DC 20013-7082
3. The National Technical Information Service, Springfield, VA 22161

Although the listing that follows represents the majority of documents cited in NRC publications, it is not intended to be exhaustive.

Referenced documents available for inspection and copying for a fee from the NRC Public Document Room include NRC correspondence and internal NRC memoranda; NRC Office of Inspection and Enforcement bulletins, circulars, information notices, inspection and investigation notices; Licensee Event Reports; vendor reports and correspondence; Commission papers; and applicant and licensee documents and correspondence.

The following documents in the NUREG series are available for purchase from the GPO Sales Program: formal NRC staff and contractor reports, NRC-sponsored conference proceedings, and NRC booklets and brochures. Also available are Regulatory Guides, NRC regulations in the *Code of Federal Regulations*, and *Nuclear Regulatory Commission Issuances*.

Documents available from the National Technical Information Service include NUREG series reports and technical reports prepared by other federal agencies and reports prepared by the Atomic Energy Commission, forerunner agency to the Nuclear Regulatory Commission.

Documents available from public and special technical libraries include all open literature items, such as books, journal and periodical articles, and transactions. *Federal Register* notices, federal and state legislation, and congressional reports can usually be obtained from these libraries.

Documents such as theses, dissertations, foreign reports and translations, and non-NRC conference proceedings are available for purchase from the organization sponsoring the publication cited.

Single copies of NRC draft reports are available free, to the extent of supply, upon written request to the Office of Information Resources Management, Distribution Section, U.S. Nuclear Regulatory Commission, Washington, DC 20555.

Copies of industry codes and standards used in a substantive manner in the NRC regulatory process are maintained at the NRC Library, 7920 Norfolk Avenue, Bethesda, Maryland, and are available there for reference use by the public. Codes and standards are usually copyrighted and may be purchased from the originating organization or, if they are American National Standards, from the American National Standards Institute, 1430 Broadway, New York, NY 10018.

DISCLAIMER NOTICE

This report was prepared as an account of work sponsored by an agency of the United States Government. Neither the United States Government nor any agency thereof, or any of their employees, makes any warranty, expressed or implied, or assumes any legal liability of responsibility for any third party's use, or the results of such use, of any information, apparatus, product or process disclosed in this report, or represents that its use by such third party would not infringe privately owned rights.

NUREG/CR-5433
SAND89-1951
R3, R4, R7

Validation of Models of Gas Holdup in the CORCON Code

Manuscript Completed: October 1989
Date Published: December 1989

Prepared by
J. E. Brockmann, F. E. Arellano, D. A. Lucero,

Sandia National Laboratories
Albuquerque, NM 87185

Prepared for
Division of Systems Research
Office of Nuclear Regulatory Research
U.S. Nuclear Regulatory Commission
Washington, DC 20555
NRC FIN A1832

ABSTRACT

Gas holdup data for oleic acid at 291 K and for 1018 steel at 1823 K has been taken for nitrogen sparging gas. The liquid levels have been measured using a real time x-ray technique. The data have been compared to correlations from the literature to assess the appropriate correlations for use in calculating gas holdup for molten core debris in reactor accident calculations. A suitable correlation has been determined as well as coefficients for use in a drift flux model. The correlation is in the form

$$\alpha = 0.128 M^{-0.0207} j_g^{*0.584}$$

where α is holdup, M is the Morton Number and j_g^* is the dimensionless gas flux through the liquid.

LIST OF FIGURES

	<u>PAGE</u>
1. Schematic Diagram of the Holdup Experimental Test Setup.....	12
2. Schematic Diagram of the WITCH/GHOST Test Article.....	14
3. Schematic Diagram of the Gas Control Manifold.....	15
4. Graph of Oleic Acid Holdup as a Function of Nitrogen Sparging Gas Face Velocity.....	20
5. Graph of 1018 Steel Holdup Data as a Function of Nitrogen Sparging Gas Face Velocity.....	25
6. Graph of Oleic Acid Holdup Data as a Function of Nitrogen Sparging Gas Face Velocity Compared to the Correlations Cited in Section 2.0.....	29
7. Graph of 1018 Steel Holdup Data as a Function of Nitrogen Sparging Gas Face Velocity Compared to the Correlations Cited in Section 2.0.....	30
8. Graph of Oleic Acid and 1018 Steel Holdup Data as a Function of the Dimensionless Face Velocity Compared to the Fit to Equation (36).....	32
9. Graph of Oleic Acid and 1018 Steel Holdup Data as a Function of the Dimensionless Face Velocity Compared to the Fit to Equation (16).....	35

CONTENTS

	PAGE
1. INTRODUCTION.....	1
2. HOLDUP.....	2
3. HOLDUP EXPERIMENTS.....	10
3.1 WITCH/GHOST Apparatus.....	11
3.2 Oleic Acid Test and Results.....	16
3.3 Steel Test and Results.....	21
4. ANALYSIS AND CONCLUSIONS.....	24
REFERENCES.....	36

LIST OF TABLES

	<u>PAGE</u>
1. Values of C_1 to be used in the Churn Flow Drift Flux Model Proposed by Gonzales [10].....	10
2. Calibrations of Critical Orifices and Upstream Pressure Transducer Used in Oleic Acid Holdup Test.....	17
3. Data From Oleic Acid Holdup Test.....	19
4. Calibration of Critical Orifices and Upstream Pressure Transducer Used in the 1018 Steel Test...	23
5. Data From 1018 Steel Holdup Test.....	24
6. Liquid and Gas Properties and Calculated Quantities for the Oleic Acid Holdup Tests.....	26
7. Liquid and Gas Properties and Calculated Quantities for the 1018 Steel Holdup Tests.....	27
8. Values of a , b , and c for Equation (36) to fit the Oleic Acid and Steel Holdup Data and Given By Renjun et al. [12].....	31
9. Values of C_0 and C_1 for Equation (16) to fit the Oleic Acid and Steel Holdup Data and Given by Blottner [6] and Gonzales [10].....	33

ACKNOWLEDGMENT

The authors wish to acknowledge the assistance and contributions of John Murray and Harold Gough of the Non-Destructive Test Division for their operation of the X-ray diagnostic equipment, Tom Kerley for his assistance in the operation of the induction furnace, and Bruce Hanshe and Kyle Thompson of the Non-Destructive Test Division for their contribution in image enhancement of the video records.

1. INTRODUCTION

As a gas bubbles up through a liquid, the level of the gas-liquid mixture rises to accommodate the gas volume mixed with the liquid volume. This phenomenon is referred to as level swell or holdup. The level swell of molten core debris as it is sparged by gas evolved from a molten core concrete interaction in a severe reactor accident has a direct effect on the core debris heat balance and on the vaporization release of radionuclides [1,2,3].

As holdup increases, the residence time of the sparging gas in the molten core debris increases. This allows greater time for vaporizing species to reach the equilibrium vapor pressure in the gas. Vaporization release will be most affected by holdup when the equilibrium vapor pressure of the vaporizing specie is not reached during the gas' transit of the melt. This will occur when the melt depth is low or when the vaporization rate is low such as would be the case with low condensed phase specie concentration [1].

Perhaps of greater significance is the effect of holdup on the overall heat balance of the molten core debris and the attack of the debris pool on vertical boundaries. The melt-concrete interaction code CORCON [2] includes the enhancement of sidewall heat transfer produced by gas sparging. The increased sidewall heat transfer coefficient along with the increased sidewall surface area resulting from level swell gives a significantly larger sideways heat flux than would arise from an unsparged melt. This is a very important consideration when evaluating melt attack on vertical structures such as pedestals or containment liners during a severe accident. The effect of holdup on heat transfer is included in the energy balance and holdup should be modeled accurately.

There are a number of correlations for holdup in the literature. They have been reviewed by Powers et al. [1] and by Kataoka and Ishii [4,5]. The data on which these correlations are based are from air-water, steam-water, and similar systems. No data for gas sparged high temperature melts have been found by the authors. The correlations of Blottner [6], Kataoka and Ishii [4], Wilson et al. [7], Sterman [8], Hughmark [9], Gonzales [10], and Renjun et al.

[12] contain fluid and gas property dependencies but give different results when applied to molten core debris. There is a need for prototypical data against which to test the various correlations.

In this paper, holdup data from an oleic acid-nitrogen system and a 1018 steel-nitrogen system are presented. These data are compared to the available correlations and a correlation is suggested for use in severe accident evaluation codes.

2. HOLDUP

The volume increase in a gas sparged liquid arising from the presence of the gas in the gas-liquid mixture is called level swell or holdup. This nomenclature comes from the increase in the height or level of the liquid in a vertical walled container during gas sparging. Holdup may also be thought of as the gas volume fraction, α , of the liquid gas mixture.

Holdup is directly related to the gas flux through the liquid, i.e., volumetric gas flow per unit surface area normal to flow. This is a face velocity, V_f , or average gas velocity normal to the surface of the liquid. In the liquid, the average gas velocity in the void regions may be thought of as the bubble rise velocity, V_B . Bubble rise velocity and face velocity are related by holdup in a steady-state system as

$$V_B = \frac{V_f}{\alpha} \quad (1)$$

In the drift flux model, the bubble rise velocity V_B is related to the terminal rise velocity, V_T , of a single isolated bubble in a stagnant pool by

$$V_B = (1-\alpha)^{n-1} V_T \quad (2)$$

where for ideal bubble flow, $n = 2$, and for churn turbulent bubble flow, $n = 0$ [6,10]. These two equations are the basis for a model of holdup. Coupled with a suitable expression for the isolated bubble terminal rise velocity V_T , an expression for holdup as a function of face velocity

and fluid properties may be written. Of course, the flow regime, ideal bubble to churn turbulent bubble, influences the model, as will the bubble size through the selection of the terminal velocity V_T .

Cole et al. [2] determine V_T based on bubble size which is determined from a stability criterion for bubble formation from a gas film. The bubble equivalent sphere diameter is given as [2,6]

$$D_B = C \left[\frac{4\sigma_1}{g(\rho_1 - \rho_g)} \right]^{1/2} \quad (3)$$

where σ_1 is the surface tension of the liquid,
 ρ_1 is the density of the liquid,
 ρ_g is the density of the gas,
 g is the gravitational acceleration, and
 C is a constant ranging from 2.2 to 3.97 [6].

However, according to Blottner [6], the face velocity required to establish a gas film is higher than the velocities covered in this work. Correlations giving the diameter of a bubble formed by gas flowing upward into a liquid from an orifice in a horizontal plate are given in Clift, Grace and Weber [11]. This is descriptive of the test geometry and systems studies in this work. The bubble equivalent sphere diameter, D_B , is given as [11]

$$D_B = \left[\frac{6}{\pi} \cdot \frac{V'}{\frac{(\Delta\rho g)}{d_{or} \sigma_1}} \right]^{1/3} \quad (4)$$

where V' is the dimensionless bubble volume

$$V' = 1.378 \cdot (Q')^{1.2} \quad (5)$$

where Q' is the dimensionless flow through the orifice

$$Q' = \left[\frac{\Delta \rho}{d_{or} \sigma_1} \right]^{5/6} g^{1/3} Q \quad (6)$$

where $\Delta \rho$ is the density difference between the liquid and the gas,

d_{or} is the orifice diameter, and

Q is the volumetric gas flow through the orifice.

This correlation holds when the dimensionless liquid viscosity μ' ,

$$\mu' = \frac{\mu_1}{(\rho_1 d_{or} \sigma_1)^{1/2}} \quad (7)$$

is less than 0.2, where μ_1 is the liquid viscosity, a condition that holds for this work.

The bubble terminal rise velocity can be calculated from a correlation given in Clift, Grace and Weber [11] for conditions in which the Morton number, M , is less than 0.001, the Eotvos number, E_o , is less than 40, and the bubble Reynolds number, Re , is greater than 0.01. This correlation applies to non-pure systems, which means only that extraordinary measures to ensure cleanliness and purity have not been taken. This is the case in our application and thus the correlation for "non-pure" systems is used. The definitions of M , E_o , and Re are

$$M = \frac{g \mu_1^4 \Delta \rho}{\rho_1^2 \sigma_1^3} \quad (8)$$

$$E_o = \frac{g \Delta \rho D_B^2}{\sigma_1} \quad (9)$$

$$Re = \frac{\rho_1 V_T D_B}{\mu_1} \quad (10)$$

where V_T is the bubble terminal rise velocity.

The correlation relates Reynolds number, which contains V_T , to a dimensionless variable J and to the Morton Number as

$$Re = (J - 0.857)M^{-0.149} \quad (11)$$

where

$$J = \begin{cases} 0.94 \cdot H^{0.757} & 2 < H < 59.3 \\ 3.42 \cdot H^{0.441} & H > 59.3 \end{cases} \quad (12)$$

and

$$H = \frac{4}{3} Eo \cdot M^{-0.149} \left[\frac{\mu_1}{\mu_w} \right]^{-0.14} \quad (13)$$

where μ_w is the viscosity of water.

This correlation yields fairly constant bubble rise velocity over the range of gas flux and bubble diameter studied in this work for each of the liquids. Thus, for the work considered here, the isolated bubble terminal rise velocity will be expressed, as in Gonzales [10] as

$$V_T = C_1 \left[\frac{\sigma_1 g \Delta \rho}{\rho_1^2} \right]^{1/4} = C_1 \left[\frac{\sigma_1 g}{\rho_1} \right]^{1/4} \quad (14)$$

Combining equations (1), (2) and (14) yields a model of holdup based on two phase flows. This drift flux model gives for ideal bubble flow ($n = 2$):

$$\alpha = \frac{1}{2} - \left[\frac{1}{4} - \frac{j_g^*}{C_1} \right]^{1/2} \quad (15)$$

and for churn turbulent bubble flow ($n = 0$):

$$\alpha = \frac{j_g^*}{C_0 j_g^* + C_1} \quad (16)$$

$$j_g^* = \frac{V_f}{\left[\frac{\sigma_1 g}{\rho_1} \right]^{1/4}} \quad (17)$$

The constant, C_0 , is suggested by Blottner [6] to account for a nonuniform distribution of bubbles across the vessel. This may be as high as 1.5 for a pipe, declining to 1.0 as the distribution of bubbles becomes uniform. This form of equation indicates that the observed holdup in a vessel with a nonuniform distribution of bubbles, e.g., a nonuniform gas flux, will be lower than in a vessel with a uniform distribution.

It is not obvious that vessel diameter correlates positively with uniformity of bubble distribution or gas flux. Empirical correlations discussed below show an inverse relationship between holdup and vessel diameter.

The correlation of Sterman [8] relates holdup produced by bubbling of steam through liquid.

The correlation given is

$$\alpha = 1.07 \left[\frac{\rho_g}{\rho_l} \right]^{0.17} D^{*-0.25} j_g^{*0.8} \quad (18)$$

where

$$D^* = \frac{D}{\sqrt{\frac{\sigma}{g(\rho_l - \rho_g)}}} \quad (19)$$

and D is the vessel diameter.

Wilson et al. [7] also give a correlation for steam rising through saturated water. They describe two regimes: one for

$$j_g^*/\alpha < 5.5$$

$$\alpha = 0.488 \left[\frac{\rho_g}{\rho_l - \rho_g} \right]^{0.115} D^{*-0.068} j_g^{*0.640} \quad (20)$$

and one for $j_g^*/\alpha > 5.5$

$$\alpha = 0.851 \left[\frac{\rho_g}{\rho_l - \rho_g} \right]^{0.180} D^{*-0.107} j_g^{*0.438} \quad (21)$$

Kataoka and Ishii [4] give an average expression for the correlation of Wilson et al. [7].

$$\alpha = 0.68 \left[\frac{\rho_g}{\rho_l} \right]^{0.17} D^{*-0.1} j_g^{*0.62} \quad (22)$$

They also give a general form for the correlation of holdup to face velocity as [4,5]

$$\alpha = N_0 \left[\frac{\rho_g}{\rho_l} \right]^{N_1} D^{*-N_2} j_g^{*N_3} \quad (23)$$

where

N_0 = the proportionality constant

N_1 = 0.1 - 0.23

N_2 = 0.1 - 0.25

N_3 = 0.62 - 0.80.

Kataoka and Ishii [4] recommended the following correlation which includes the viscosities of the liquid and gas:

$$\alpha = 0.67 \left[\frac{\rho_g}{\rho_l} \right]^{2/9} D^{*-1/6} j_g^{*2/3} \left[\frac{\mu_g}{\mu_l} \right]^{-2/9} \quad (24)$$

Hughmark [9] gives a correlation in which the face velocity is normalized by the deviation of fluid properties from those of water. The equation is from Powers et al. [1]

$$\alpha = \exp[-3.5349 + 0.9358 \ln \beta - 0.06553 (\ln \beta)^2] \quad (25)$$

where

$$\beta = V_f \left[\frac{\rho_w}{\rho_l} \cdot \frac{\sigma_w}{\sigma_l} \right]^{1/3} \quad (26)$$

ρ_w is the density of water at room temperature and
 σ_w is the surface tension of water at room
 temperature

and V_f is in units of cm/s.

Renjun et al. [12] propose the following correlation which depends on dimensionless gas flux, Morton number and the saturation vapor pressure of the liquid.

$$\alpha = 0.1966 M^{-0.0070} \left[\frac{(P+P_s)}{P} \right]^{1.6105} j_g^{*0.5897} \quad (27)$$

where P is the ambient total pressure and P_s is the saturation vapor pressure of the liquid.

Except for Renjun et al. [12] and Hughmark [9], these correlations display an inverse relationship between holdup and vessel diameter. Gonzales [10] indicates that for $D^* > 30$, vessel diameter has no effect on holdup and does not include the parameter in his model.

This model is a drift flux model in which the coefficients are determined by correlations to data. While D^* is not included in the correlations, a viscosity parameter is. It is defined as

$$N_\mu = \frac{\mu_l}{\left[\rho_l \sigma \left[\frac{\sigma}{g \Delta \rho} \right]^{1/2} \right]^{1/2}} \quad (28)$$

which is the Morton Number to the 1/4 power, $M^{1/4}$.

Gonzales [10] gives as his model

$$\alpha = \frac{j_g^*}{\left[C_0 j_g^* + C_1 (1-\alpha)^n \right]} \quad (29)$$

where $C_0 = 1.2$ and C_1 is given by the following experimentally determined correlations.

For bubble flow, $j_g^* < 0.4$ and $n = 1.75$,

if $M < 2.6 \cdot 10^{-10}$, then

$$C_1 = 0.83 \left[\frac{\rho_g}{\rho_l} \right]^{0.207} M^{-0.0928} \quad (30)$$

and if $M > 2.6 \cdot 10^{-10}$, then

$$C_1 = 0.00073 \left[\frac{\rho_g}{\rho_l} \right]^{-1.412} \quad (31)$$

For Churn flows, $j_g^* > 0.4$ and $n = 0$, if

$M < 2.6 \cdot 10^{-10}$, then

$$C_1 = 1.8 \left[\frac{\rho_g}{\rho_l} \right]^{.541} M^{-0.1638} \quad (32)$$

and if $M > 2.6 \cdot 10^{-10}$, then

$$C_1 = 7.4 \left[\frac{\rho_g}{\rho_l} \right]^{0.106} \quad (33)$$

This model generates values for C_1 which may be considerably different than are employed in the drift flux model described by Blottner [6] and used in CORCON [2]. Blottner suggests, for churn flow, a value of $C_0 = 1.0$ and $C_1 = 1.99$. Gonzales [10] suggests a value of $C_0 = 1.2$ and gives system dependent values for C_1 . Table 1 lists some of these experimentally determined values and the values determined by correlation.

TABLE 1

Values of C_1 to be used in the Churn Flow Drift Flux Model Proposed by Gonzales [10].

$$C_0 = 1.2$$

<u>Liquid</u>	<u>Experimental Value</u>	<u>Correlation Result</u>
Water	2.63	2.56
Freon 113	1.52	1.47
Freon 11	1.74	1.86
Mercury	2.27	2.26
Silicone Oil	3.65	3.65
Tetrabromoethane	3.25	3.25

This approach, to experimentally determine the coefficients for the drift flux model, will be used along with comparison to the correlations cited here to examine the experimentally measured holdup of oleic acid sparged by nitrogen and of molten 1018 steel sparged by nitrogen.

3. HOLDUP EXPERIMENTS

Experiments were performed in the WITCH/GHOST apparatus [3] to determine holdup for oleic acid sparged with nitrogen at 291 K and for a 1018 steel sparged with nitrogen at 1823 K. These data were obtained to provide a validation of the holdup correlation used in CORCON [2] and VANESA [1]. The oleic acid tests provided a means to evaluate and check the experimental apparatus and technique. These tests also generated data which could be readily compared with

correlations based on data from similar systems. The steel data represents a set of unique holdup measurements made on molten steel and provides the most prototypic data base for application to reactor accident conditions.

The experimental technique involves the real-time x-ray observation of the level swell of a gas sparged liquid. The liquid is contained in a right cylindrical crucible with a sparger plate bottom. A video tape record is made of the x-rays of melt holdup for various gas sparging rates. Figure 1 shows a schematic diagram of the holdup experimental test setup. Shown is the WITCH/GHOST test article, the sparging gas control system, the x-ray source and the real-time video imaging system.

3.1 WITCH/GHOST Apparatus

The test article has been designed to contain a liquid while it is being sparged with gas. It consists of a cylindrical crucible with a flat sparger plate bottom. This crucible fits into a pedestal which acts as a plenum for the sparging gas. The test article is cast from a castable ceramic material (Alundum CA331 from Norton Refractories Division) in three pieces: the crucible sleeve, the sparger plate and the pedestal. After drying, these three pieces are cemented together with the wet alumina ceramic, dried, and then fired according to the manufacturer's specifications to 1000°C.

The ceramic was selected to allow study of inductively melted and sustained high temperature melts and for its relatively high x-ray transmissivity.

The sleeve is cast in the annular region between two right circular cylinder forms. The nominal dimensions of the casting are 20.3 cm outer diameter, 16.2 cm inside diameter and 86 cm length.

The sparger plate is cast as a 3 cm thick disk with approximately one 0.08 cm diameter hole per square cm. The form for the casting consists of a short right cylinder with an inside diameter of about 20 cm. Two plates with matching hole patterns cover either end of the cylinder and 0.08 cm diameter wires are strung through the matching holes. The

TEST SETUP

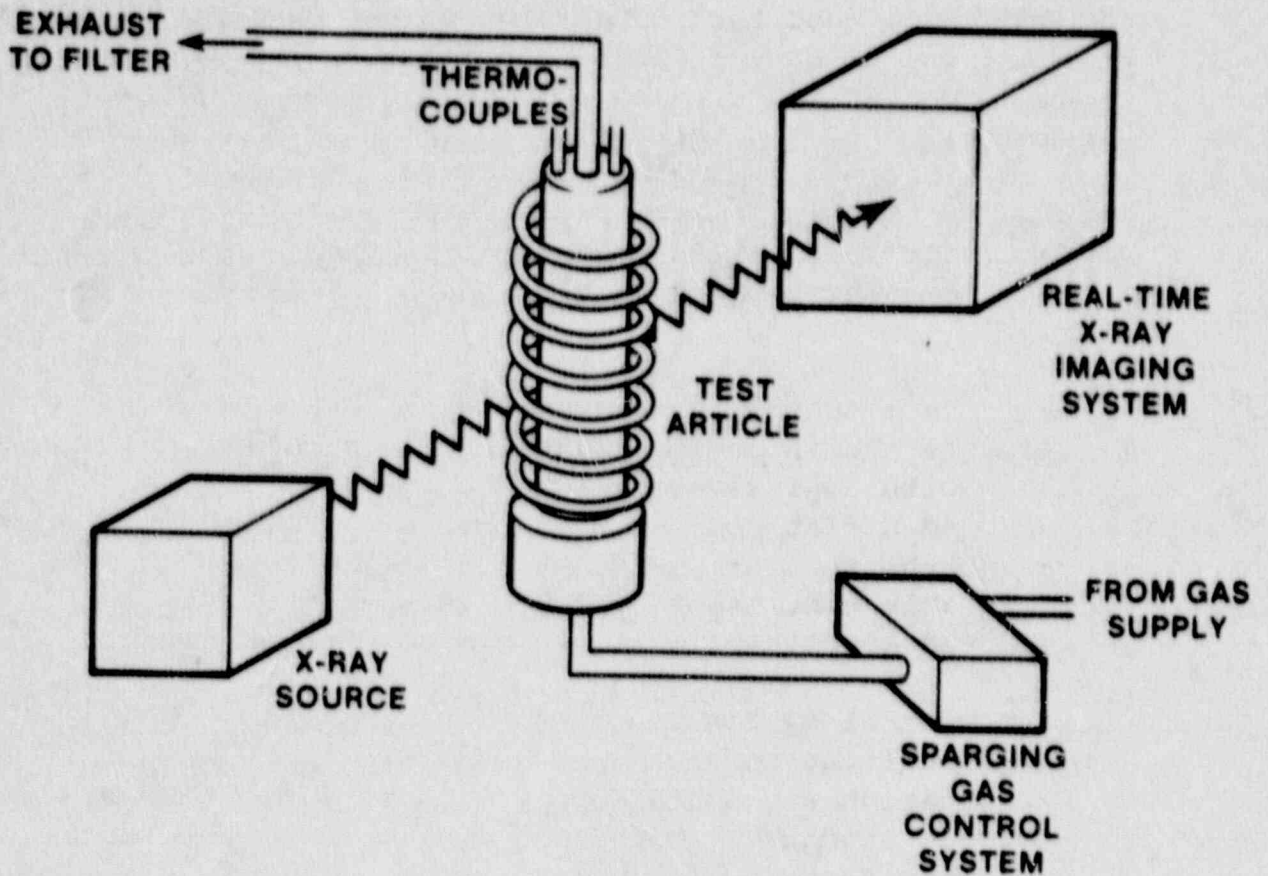


Figure 1. Schematic Diagram of the Holdup Experimental Test Setup

castable ceramic is poured into the form and allowed to set. The wires are then removed and the plate taken from the form.

The pedestal is cast using a 25 cm inside diameter cylindrical form about 15 cm high. The internal features are made by a wood form consisting of two concentric 2.5 cm thick disks, 21 cm and 15.5 cm in diameter. A 2.5 cm ceramic tube is centered on the smaller disk and this assembly centered in the cylindrical form with the larger disk resting on a Plexiglass plate and the ceramic tube protruding through the top plate which rests on the 25 cm diameter form. Castable ceramic is poured through holes in this plate. The casting is allowed to set and the forms are removed.

Figure 2 is a schematic diagram of the test article shown in relation to the induction coils. The finished piece is a crucible with approximately a 16 cm inside diameter, a 1.9 cm wall and a flat sparger plate bottom. The depth is about 85 cm and the sparger plate has a hole density of $1/\text{cm}^2$. This crucible contains the liquid (either oleic acid or molten 1018 steel) while it is sparged with nitrogen.

The gas control system consists of a manifold of four critical orifices connected in parallel which may be used in any combination and a gas supply with an adjustable pressure regulator. At choked flow (when the upstream pressure is more than twice that of the downstream pressure) a critical orifice gives a constant volumetric flow of gas at the upstream conditions. Consequently, by varying the upstream pressure, the mass flow of gas can be varied. Upstream and downstream temperature and pressure are monitored and pretest calibration of the orifices and transducers enable measurement and control of the sparging gas entering the crucible. Figure 3 is a schematic diagram of the gas control manifold.

WITCH/GHOST TEST ARTICLE

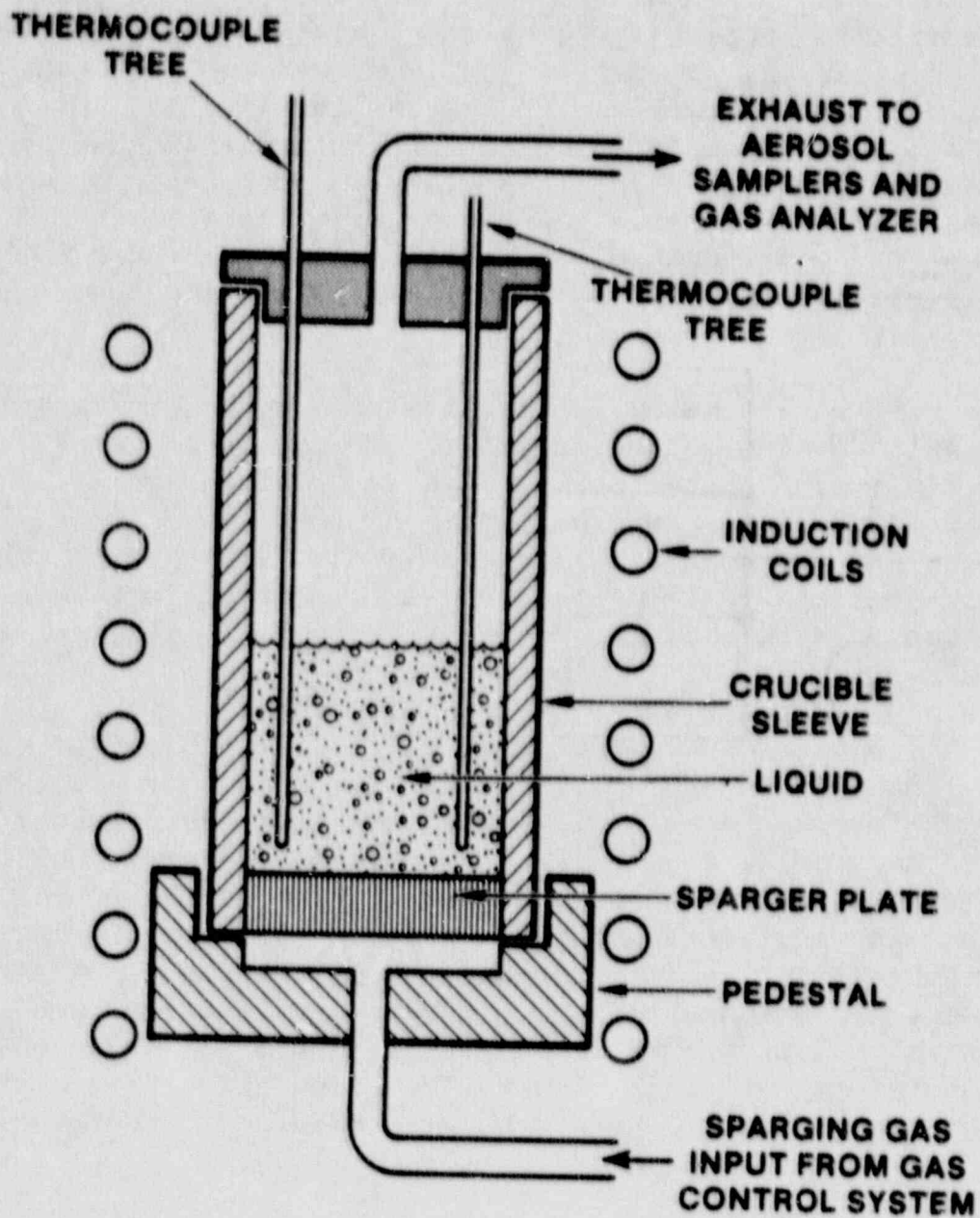


Figure 2. Schematic Diagram of the WITCH/GHOST Test Article

GAS CONTROL MANIFOLD

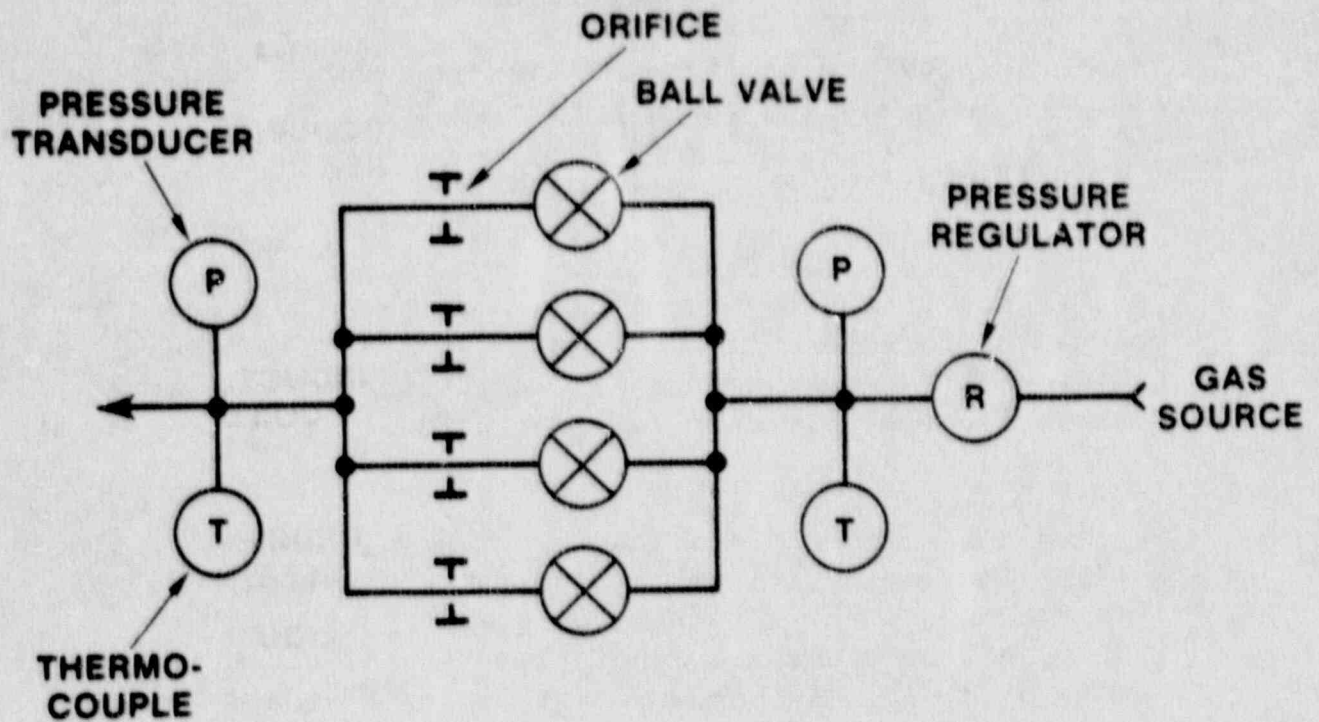


Figure 3. Schematic Diagram of the Gas Control Manifold

Real-time x-ray video records of the liquid level are taken to determine the level swell produced by gas sparging. An x-ray source is directed through the test article and the image formed on a phosphorus screen. This image is photographed by a video camera and monitored and recorded.

The test with oleic acid as the liquid employed a Linatron as the x-ray source (5 to 10 MeV x-rays at 1000 R/min at 1 meter) and the high temperature 1018 steel test used a portable ^{60}Co source (1.2 MeV at about 700 R/hr at 1 meter).

Figure 1 shows the relation of the gas supply, test article, and x-ray diagnostics for a holdup test.

3.2 Oleic Acid Test and Results

In order to test the feasibility of this technique, a test article was built and used to measure the holdup of nitrogen sparged oleic acid at 25°C. The x-ray source used was the Linatron operated by Sandia National Laboratories' Non-Destructive Test Division I. It produces 5 to 10 MeV x-rays at about 1000 R/min at 1 meter.

Because the sparger plate has holes through which the liquid can leak out unless there is a positive gas flow, the unsparged liquid height is calculated from the volume of liquid and the cross-sectional area of the crucible. The volume of oleic acid used was 4.6 liters \pm 5% and the crucible cross-section was 198 cm² \pm 2% (15.9 cm \pm 1.5% diameter). This gives an unsparged height of oleic acid of 23.2 cm \pm 5.4%.

The face velocity of the sparging gas is calculated from the volumetric gas flow at the liquid surface conditions divided by the crucible cross-sectional area. The volumetric flow is known to better than \pm 3.3% and the face velocity has an accuracy of better than \pm 3.8%.

The calibrations for the critical orifices and upstream pressure transducer used in the oleic acid holdup test are given in Table 2.

TABLE 2

Calibrations of Critical Orifices and
Upstream Pressure Transducer Used
in Oleic Acid Holdup Test.

<u>Orifice Designation</u>	<u>Flow</u> <u>(cm³/s)</u>
14R	283.3 ± 2.2%
14B	250.7 ± 1.4%
10	160.5 ± 2.0%

Pressure transducer - mV output
P(PSIA) = 1.3445 (mV) - 3.417
Uncertainty in P is ± 2%

The sparged liquid height (distance from sparger plate to liquid surface) was measured from the screen of the video monitor. Because the unsparged height cannot be recorded on the screen, a conversion from screen height to actual height is required. Three lead bricks of a height of 15.24 cm were recorded with the same x-ray diagnostic as the liquid level. On the screen they measured 5.2 cm giving a conversion of 2.93 actual cm per screen cm.

The liquid height could be measured to ± 2 mm on the screen and the observed liquid height on the screen was on the order of 8 cm giving an uncertainty in observed liquid height of ± 2.5%. This uncertainty was caused in part by variation of the observed level about a mean value and the uncertainty reflects the uncertainty in determining the mean level.

The holdup, α , is calculated as

$$\alpha = \frac{(h - h_o)}{h} \quad (34)$$

where h is the observed liquid height and
 h_o is the unsparged liquid height.

The uncertainty in α arising from the uncertainties in h and h_o is defined as

$$U(\alpha) = \left[\frac{h_o/h}{\alpha} \right] \left[U(h)^2 + U(h_o)^2 \right]^{1/2} \quad (35)$$

where $U(x)$ denotes the uncertainty in x and is expressed as a percentage or fraction of x .

Fourteen holdup data points were taken for face velocities ranging from 4.5 cm/s to 30 cm/s. These data are presented in Table 3.

The table gives the upstream pressure, P_u , as the transducer voltage and in psia; the volumetric flow rate upstream of the critical orifices, Q_{oc} ; the face velocity, V_f , at the liquid surface; the observed liquid height, h , in actual cm; the holdup, α ; and the uncertainty in α , $U(\alpha)$, in the same units as α .

Figure 4 is a graph of the oleic acid holdup as a function of the nitrogen sparging gas face velocity.

TABLE 3

Data from Oleic Acid Holdup Test

Oleic Acid, 291 K

Crucible Cross-Section = 198 cm² ± 2%

Liquid Volume = 4.20 liters ± 5%

Unsparged Liquid Depth h_0 = 21.2 cm ± 5.4%

P_u	Q_{oc}	V_f	h	a	$U(a)$	
(mV)	(psia)	(cc/sec)	(cm/s)	(cm/cm)	(cm/cm)	
36.44	45.56	238.3	4.50	22.7	.066	.056
44.05	55.81	238.3	5.52	23.5	.098	.054
55.33	70.97	238.3	7.01	23.8	.109	.053
62.90	81.15	238.3	8.02	24.1	.120	.052
24.71	29.81	649.5	8.01	23.8	.109	.053
35.85	44.78	649.5	12.04	24.7	.142	.051
46.70	59.37	649.5	15.96	25.6	.172	.049
69.03	89.39	649.5	24.0	26.2	.191	.048
85.61	111.7	649.5	30.3	27.5	.229	.046
69.02	89.38	649.5	24.0	27.4	.226	.046
46.60	59.24	649.5	15.92	24.6	.138	.051
24.76	29.87	649.5	8.03	23.8	.109	.053
55.40	71.07	238.3	7.01	23.5	.098	.054
44.08	55.85	238.3	5.51	23.0	.078	.055

Observed liquid height ± 2.5%

 V_f ± 3.8%

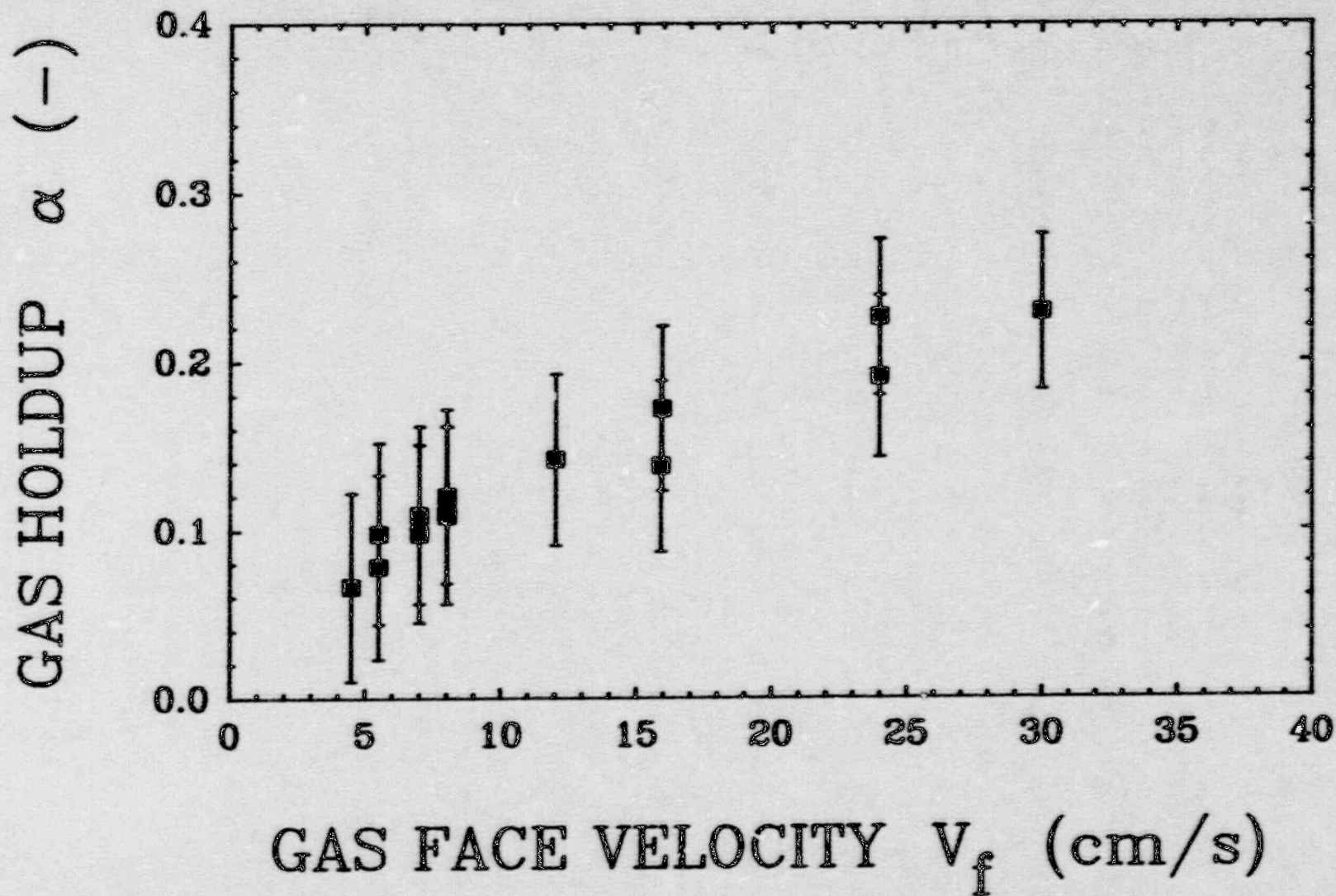


Figure 4. Graph of Oleic Acid Holdup as a Function of Nitrogen Sparging Gas Face Velocity

3.3 1018 Steel Test and Results

In this test, 1018 mild steel at 1823 ± 25 K was sparged with nitrogen and the gas holdup measured. The x-ray source used was a ^{60}Co source operated by Sandia National Laboratories' Non-Destructive Test Technology Division I. It produces 1.2 MeV x-rays at about 700 R/hr at 1 meter.

The crucible was instrumented with thermocouples. To measure melt temperatures, 1.27 cm diameter closed end alumina thermowells were placed along the wall inside the crucible. Type-S platinum-rhodium thermocouples sheathed in 0.32 cm double bore alumina tubing with the junction exposed were placed inside the thermowell with the junctions all toward the same side. The remaining void was potted with castable ceramic and fired. The thermowells were placed so that the sides with the thermocouple beads were oriented toward the center of the crucible. Four thermowells were placed on this test: two with 3 Type-S thermocouples each located 180° apart with the thermocouples located at 5.1 cm, 10.2 cm, and 20.3 cm above the sparger plate and two with 2 Type-S thermocouples located 180° apart and 90° from each of the other thermowells with the thermocouples located at 7.6 cm and 15.2 cm above the sparger plate.

Type-K thermocouples were placed on the outside of the crucible wall in four vertical arrays of 3 thermocouples 90° apart. They were at 7.6 cm, 20.3 cm and 27.9 cm above the level of the top of the sparger plate. The radial locations matched the radial locations of the Type-S thermocouples inside the crucible.

A thin-walled zirconia sleeve of about 30 cm diameter was placed concentrically around the crucible and the annular gap dry rammed with alumina powder. This provided mechanical support to the crucible and held the Type-K thermocouples in place.

An induction coil of 31 cm inside diameter was placed around this assembly. A 50 kW Inductotherm power supply was connected to the coil and used to inductively heat and melt a 28.6 kg 1018 mild steel charge. The charge was 15 cm in diameter with a tapered top to avoid hanging up in the crucible as the lower supporting portion of the slug melted.

The sides of the slug had machined channels to accommodate the thermowells. The heatup and melting took about 8 hours to avoid thermally stressing the crucible during heatup. A crust formed and was melted by raising the coil. An additional mass of 21.0 kg was added in the form of balls through a hole in the crucible cover to bring the total melt mass to 49.6 kg.

In order to calculate the unsparged melt height, the thermal expansion of the crucible and steel charge must be taken into account. The crucible diameter at 25°C was 16.0 cm ± 1%. Taking 1.5% as the linear thermal expansion from 25°C to 1500°C (13, 14) for the ceramic and an average crucible wall temperature of 1500°C gives a crucible inside diameter of 16.24 cm ± 1% and a cross-sectional area of 207 cm² ± 2%. The density of the steel at 25°C is 7.86 g/cm³. Taking 5.7% as the volumetric expansion of the steel up to the melting point [15] and 3.5% as the volumetric expansion on melting [16] gives a density of 7.2 g/cm³ for the molten steel. It is estimated that splash and unmelted steel adhering to the crucible walls was 1 to 3 kg. This gives a sparged liquid mass of 47.6 ± 1 kg or 6610 cm³ ± 2.1%. The thermowells account for 5 cm² of excluded area giving a final cross-sectional area of 202 cm² ± 2% and an unsparged melt height of 32.7 cm ± 2.9%.

The face velocity of the sparging nitrogen gas is calculated at the melt surface conditions of 1823°C and 12.1 psia. The calibrations for the critical orifices and upstream pressure transducer used in the 1018 steel holdup test are given in Table 4.

TABLE 4

Calibration of Critical Orifices and Upstream
Pressure Transducer Used in 1018 Steel Test.

<u>Orifice Designation</u>	<u>Flow (cm³/s)</u>
14	247.0 ± 2%
10	160.7 ± 2%
5	72.3 ± 2%
3	34.5 ± 2%

Pressure Transducer - mV output
P(psia) = 1.141 (mV) - 0.0296 ± 2%

The liquid height was measured from the screen of the video monitor. Because the melt depth was greater than the field of vision, the sparger plate could not be included in the video record. Instead, lead bricks 5.08 cm thick with central points were stacked alongside the coil to provide a reference. This appeared as a vertical saw tooth shape with the points 5.08 cm apart.

The quality of the video record required image enhancement. The Sandia National Laboratories' video enhancement group provided a very usable image. A few averaged frames were stored for three times during each holdup data period. Using a computer controlled image enhancement system, the difference in signals from the stored images and a stored reference image gave an image with the melt level presented in good contrast. The computerized system allowed indexing on the lead brick scale and provided a horizontal cursor which could be moved to the melt level to give a direct readout of the melt height. The uncertainty in the observed melt height is determined from the three readings taken at each holdup level and is calculated as ± 2%.

Holdup and uncertainty are calculated using equations (34) and (35). Table 5 contains the holdup data from the 1018

steel holdup test. The table gives the pressure upstream, P_u , of the critical orifices as transducer voltage and psia; the volumetric flow rate upstream of the orifices, Q_{oc} ; the face velocity, V_f , at the melt surface; the observed melt height, h ; the holdup, α ; and the uncertainty in α , $U(\alpha)$, in the same units as α .

Figure 5 is a graph of the 1018 steel holdup data as a function of the nitrogen sparging gas face velocity.

TABLE 5

Data from 1018 Steel Holdup Test

1018 steel, 1823 K \pm 25 K
 Crucible Cross-Section = 202 cm² \pm 2%
 Liquid Volume = 6610 cm³ \pm 2.1%
 Unsparged Liquid Depth h_0 = 32.74 cm \pm 2.9%

P_u	Q_{oc}	V_f	h	α	$U(\alpha)$	
(mV)	(psia)	(cc/sec)	(cm/s)	(cm/cm)	(cm/cm)	
44.1	50.3	72.3	9.3	37.06	.116	.032
52.7	60.1	72.3	11.1	38.76	.155	.030
61.5	70.1	72.3	12.9	39.09	.162	.030
75.2	85.8	72.3	15.9	40.28	.187	.029
44.1	50.3	160.3	20.6	43.46	.246	.027
52.7	60.1	160.3	24.6	45.54	.281	.026
52.7	60.1	160.3	24.6	45.14	.274	.026
61.5	70.1	160.3	28.8	47.04	.303	.025
70.2	80.1	160.3	32.8	47.32	.308	.025
52.7	60.1	247.0	37.8	49.10	.333	.024

Observed liquid height \pm 2%
 $V_f \pm$ 4%

4. ANALYSIS AND CONCLUSION

The holdup data taken with oleic acid and with 1018 steel will be compared to the models and correlations of holdup reviewed in section 2.0. In order to apply these models, properties of the liquids and gases and dimensions of the

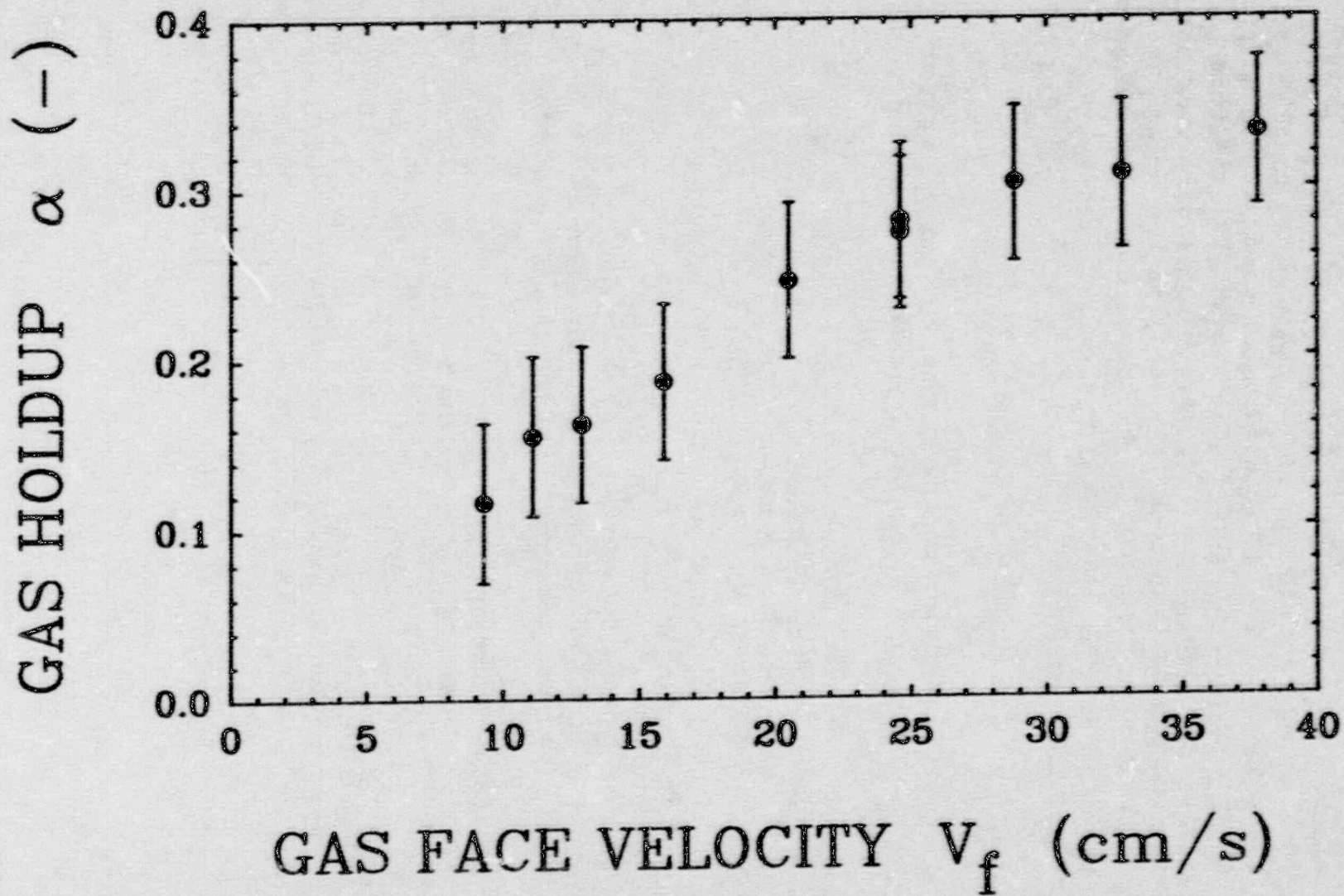


Figure 5. Graph of 1018 Steel Holdup Data as a Function of Nitrogen Sparging Gas Face Velocity

apparatus must be known. Tables 6 and 7 list this information for oleic acid and molten 1018 steel respectively. The oleic acid properties were found from the CRC Handbook of Chemistry and Physics [17] and from Baron [18]. The steel properties were taken from properties for iron in the CRC handbook [17] and from the properties listed in the VANESA Manual [1]. The properties of nitrogen were taken from Eckert and Drake [19].

TABLE 6

Liquid and Gas Properties and Calculated Quantities for the Oleic Acid and Holdup Tests

Test Conditions:

Temperature =	291 K ± 1 K
Pressure =	12.1 psia

Liquid: Oleic Acid

Density =	0.895 g/cm ³
Viscosity =	0.27 poise
Surface Tension:	32.5 dynes/cm
Vapor Pressure:	Less than 1% ambient

Gas: Nitrogen

Density =	9.65 · 10 ⁻⁴ g/cm ³
Viscosity =	1.84 · 10 ⁻⁴ poise

Quantities:

Morton Number =	1.7 · 10 ⁻⁴
-----------------	------------------------

$$\left[\frac{\sigma_1 g}{\rho_1} \right]^{1/4} = 13.7 \text{ cm/s}$$

$$D^* = 84$$

$$j_g^* = \frac{V_f}{\left[\frac{\sigma_1 g}{\rho_1} \right]^{1/4}}$$

TABLE 7

Liquid and Gas Properties and Calculated Quantities for the 1018 Steel Holdup Tests

Test Conditions:

Temperature = 1823° K ± 25 K
 Pressure = 12.1 psia

Liquid: Molten 1018 Steel

Density = 7.2 g/cm³
 Viscosity = 0.057 poise
 Surface Tension = 1100 dynes/cm
 Vapor Pressure = less than 1% ambient

Gas: Nitrogen

Density = 1.55 · 10⁻⁴ g/cm³
 Viscosity = 6.0 · 10⁻⁴ poise

Quantities:

Morton Number = 1.1 · 10⁻¹²

$$\left[\frac{\sigma_{lg}}{\rho_l} \right]^{1/4} = 19.7 \text{ cm/s}$$

$$D^* = 41$$

$$j_g^* = \frac{V_f}{\left[\frac{\sigma_{lg}}{\rho_l} \right]^{1/4}}$$

All but the lowest face velocity data point in the oleic acid data set fit Gonzales' [10] criterion for bubbly churn flow, i.e., $j_g^* > 0.4$, and all data points fit the criterion of Kataoka and Ishii [4,5], i.e., $j_g^* > 0.325$. The data will be considered to be in the churn flow regime and appropriate holdup correlations employed.

The dimensionless container diameters exceed the value of 30, beyond which Gonzales [10] indicates container diameter has no influence on holdup.

The parameter values given in Tables 6 and 7 were used to calculate the holdup from the models and correlations. These comparisons are given in Figures 6 and 7 for oleic acid and 1018 steel holdup data respectively. The holdup data are presented as functions of gas face velocity along with the correlations. The order in which the correlations are listed in the key, is the order in which the curves appear from top to bottom.

For a particular correlation to be accepted as a candidate for use in reactor accident models, it should reasonably fit the data for both oleic acid and steel. The drift flux model given by Blottner [6] and currently in use in CORCON [2] overpredicts the data for both liquids.

For the oleic acid data shown in Figure 6, Kataoki and Ishii [4] along with Blottner [6] considerably overpredict the data. Hughmark [9] generally overpredicts the data but does reproduce the slope. Gonzales [10] and Renjun et al. [12] slightly overpredict the data. Wilson et al. [7] and Sterman [8] both give rather good predictions of the data.

For the 1018 steel data, Hughmark [9], Kataoki and Ishii [4], Wilson et al. [7] and Sterman [8] underestimate the data considerably as is seen in Figure 7. Gonzales [10] severely overpredicts the data and is scarcely on the figure. Rejun et al. [12] give an excellent prediction of the data.

Only the correlation of Renjun et al. [12] does a reasonable job on both sets of data; it gives excellent agreement on the steel data and slightly overpredicts holdup for the oleic acid data. Rejun et al. [12] addressed the effects of vapor pressure in holdup and correlated data for Morton Number and dimensionless gas face velocity as well. The data were taken for air-water, air-alcohol and air-5% NaCl solution systems in a 10 cm diameter column at temperatures ranging from 25°C to 95°C. They assert that no diameter effects of the column are present. Indeed, the dimensionless vessel diameter for their work is about 40 and exceeds the criterion of 30 as given by Gonzales [10]. The

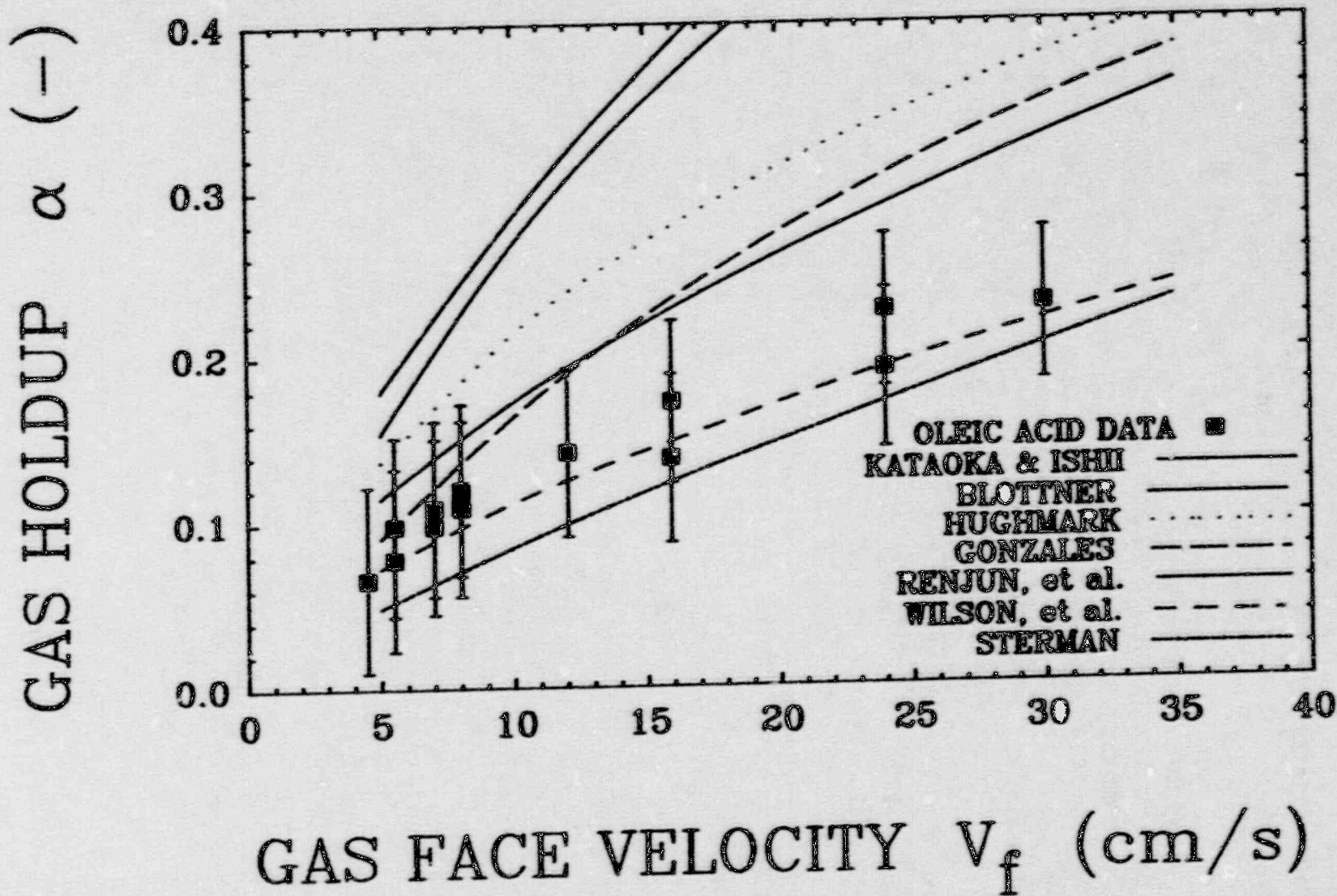


Figure 6. Graph of Oleic Acid Holdup Data as a Function of Nitrogen Sparging Gas Face Velocity Compared to the Correlations Cited in Section 2.0.

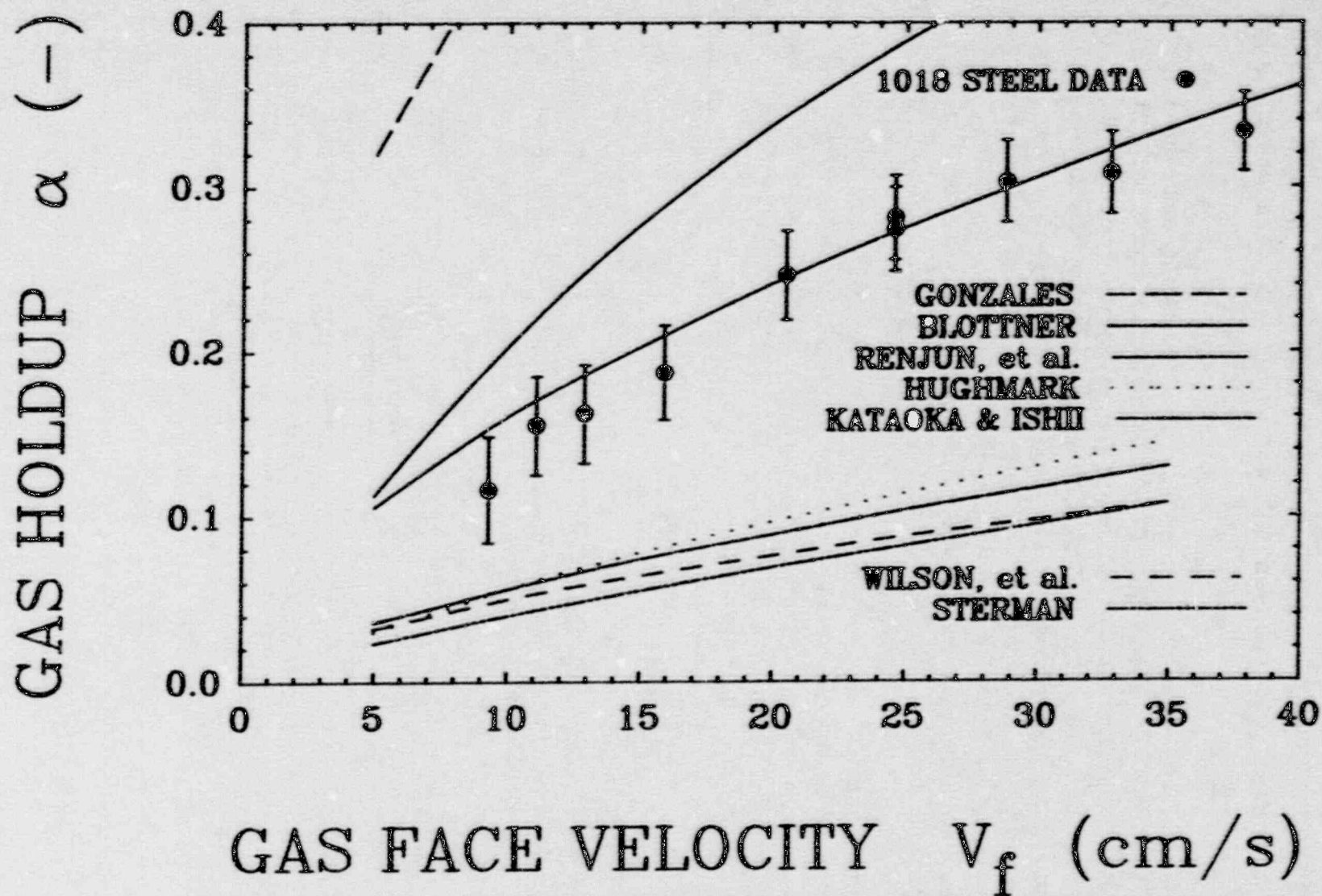


Figure 8. Graph of Oleic Acid and 1018 Steel Holdup Data as a Function of the Dimensionless Face Velocity Compared to the Fit to Equation (36).

Morton Number range of the data is from about $5 \cdot 10^{-13}$ to $5 \cdot 10^{-10}$ and encompasses that of the steel data at $1.1 \cdot 10^{-12}$.

The correlation of Renjun et al. [12] depends only on the liquid properties and gas flux through the surface. It is based on data covering a Morton range which includes that of the molten steel data. Their vessel diameter is large enough that no diameter effects should be seen on the observed holdup. Further, the correlation is not unreasonable in its prediction of the oleic acid data. For these reasons, the correlation of Renjun et al. is a good candidate for use in CORCON [2].

If the form of the Renjun et al. [12] correlation, without the vapor pressure term, is taken and the steel and oleic acid data are both fit to this form, a correlation covering a much wider range of Morton Number, 10^{-12} to 10^{-4} , is obtained. The correlation is of the form

$$\alpha = c \cdot M^a \cdot j_g^{*b} \quad (36)$$

where the values of the coefficients a, b and c from the data fit for the oleic acid and steel and from Renjun et al. [12] are given in Table 8.

TABLE 8

Values of a, b and c for Equation (36) to fit the oleic acid and steel holdup data and given by Renjun et al. [12]

	a	b	c
Present Work	-.0207	0.584	0.128
Renjun et al.	-.0070	0.5897	0.1966

Figure 8 is a graph of the holdup data from both the oleic acid and steel data sets as a function of dimensionless face velocity along with the fit of Equation (36). It is clearly seen by plotting holdup as a function of dimensionless gas

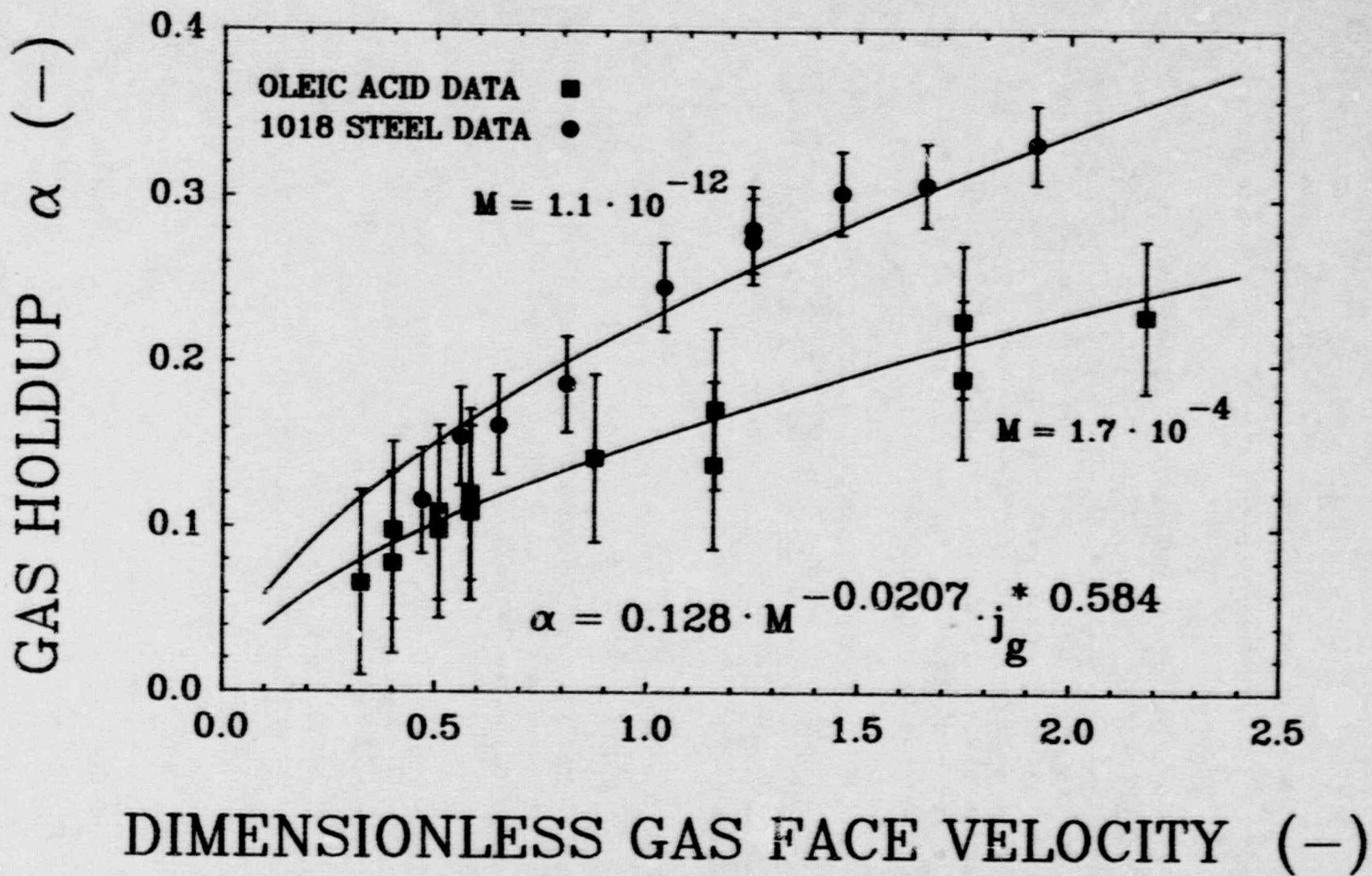


Figure 7. Graph of 1018 Steel Holdup Data as a Function of Nitrogen Sparging Gas Face Velocity Compared to the Correlations Cited in Section 2.0.

face velocity that non-dimensionalizing the face velocity in this way does not produce a universal curve. The Morton Number dependence may account for the difference in data sets.

An equation in the form of the drift flux model given in Equation (16) may be used with coefficients C_0 and C_1 determined from fits to data as an expression for holdup. This equation is

$$\alpha = \frac{j_g^*}{C_0 \cdot j_g^* + C_1} \quad (16)$$

Blottner determined the values of C_0 and C_1 from theoretical considerations and Gonzales [10] assumed a value of C_0 and presented a correlation for C_1 based on values of C_1 experimentally determined for various liquids.

The data presented here have been fit to Equation (16) and the values of C_0 and C_1 determined. Table 9 gives these fitted values as well as those given by Blottner [6] and Gonzales [10].

TABLE 9

Values of C_0 and C_1 for Equation (16) to fit the oleic acid and steel holdup data and given by Blottner [6] and Gonzales [10].

<u>Source</u>	<u>C_0</u>	<u>C_1</u>
Blottner [6]	1.0	1.99
Gonzales [10]		
Oleic Acid	1.2	3.57
Steel	1.2	0.49
This Work		
Oleic Acid	2.77	3.76
Steel	1.03	3.37
Steel w/ C_0		
Constrained	1.2	3.25

The fits of C_0 and C_1 give excellent agreement with the data and the values for steel whether C_0 is constrained to 1.2 as in Gonzales [10] or not, gives curves which are almost indistinguishable. Figure 9 shows the holdup data for oleic acid and steel plotted as a function of dimensionless gas face velocity along with the fits to Equation (16).

The different values of C_0 and C_1 accommodate Equation (16) to each set of data. Gonzales [10] did not successfully predict values of C_1 to fit the oleic acid data well or the steel data at all. The values of C_0 and C_1 selected by Blottner [6] considerably overpredict the data presented here.

The steel data is excellently predicted by Renjun et al. [12], by the fit to Equation (36) and by the fit to Equation (16). The oleic acid data is fit excellently by the fit to Equation (36) and by the fit to Equation (13). Renjun et al. [12] slightly overpredicts these data.

If Blottner [6] is modified in CORCON [2] by adjusting the coefficients to those of the steel data, it is still as property invariant as the old model. There does not appear to be an acceptable correlation to determine coefficients.

Renjun et al. [6] predicts the steel data very well and is probably good for Morton Numbers in the range of its data base. It does overestimate the oleic acid data. Renjun et al. [6] would be an acceptable substitute for Blottner in CORCON [2]. It has more property variability embodied in the Morton Number dependence.

The fit to Equation (36) predicts the steel and oleic acid data very well but is based on a limited data base. Until it is tested against other data, its use as a substitute for Blottner is recommended with caution. However, it is a good approximation for Renjun et al. [6] over the range of Morton Number they investigated and consequently should be no worse than Renjun et al. [6].

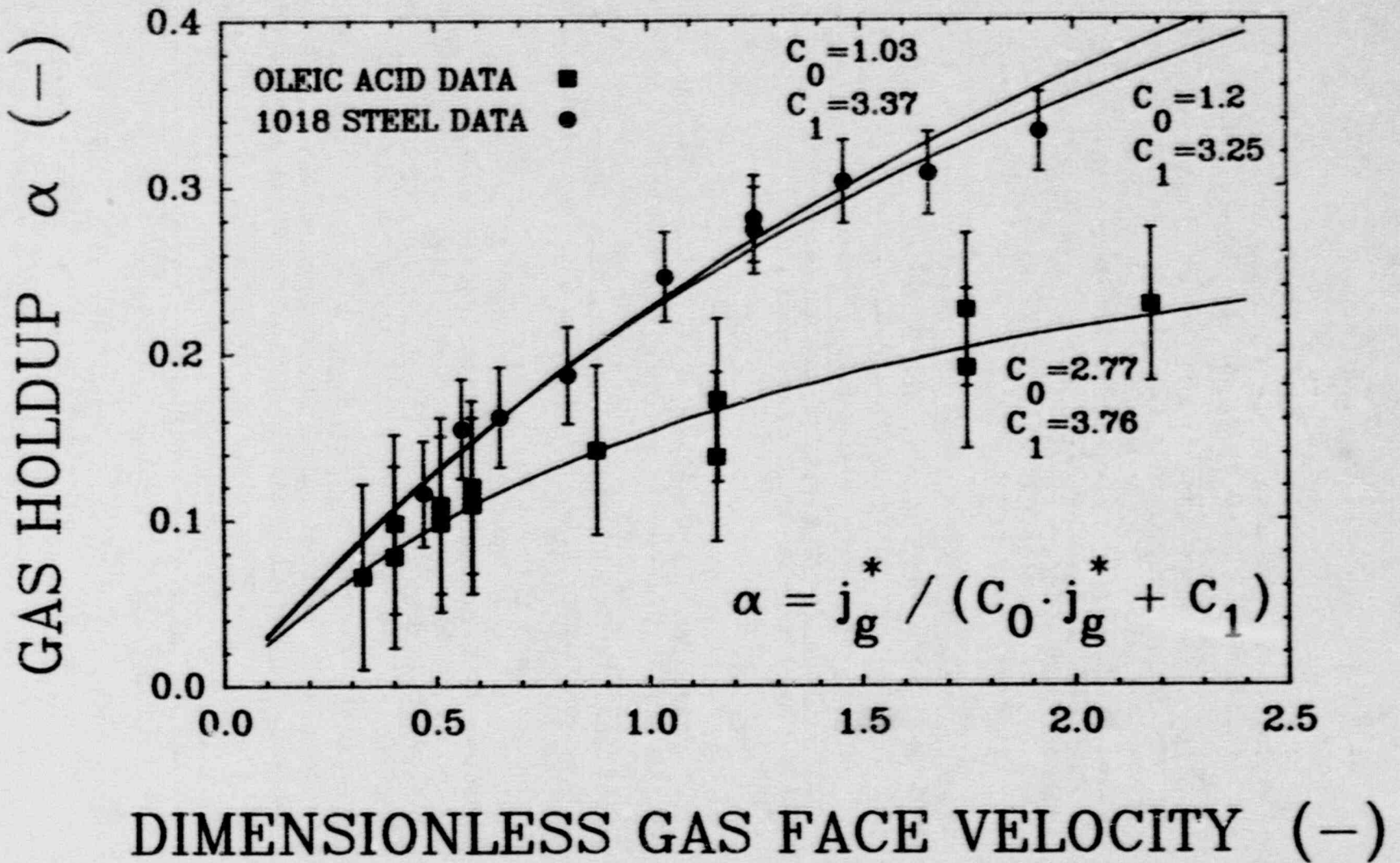


Figure 9. Graph of Oleic Acid and 1018 Steel Holdup Data as a Function of the Dimensionless Face Velocity Compared to the Fit to Equation (16).

REFERENCES

1. Powers, D. A., Brockmann, J. E. and Shiver, A. W., VANESA: A Mechanistic Model of Radionuclide Release and Aerosol Generation During Core Debris Interactions with Concrete, NUREG/CR-4308, SAND85-1370, Sandia National Laboratories, Albuquerque, NM, 1986.
2. Cole, R. K., Jr., Kelly, D. P. and Ellis, M. A., CORCON-MOD2: A Computer Program for Analysis of Molten-Core Concrete Interactions, NUREG/CR-3920, SAND84-1246, Sandia National Laboratories, Albuquerque, NM, 1984.
3. Reactor Safety Research Semi-Annual Report July-December 1987, NUREG/CR-5039, SAND87-2411, Volume 2, Section 1.2 pp 28-33 1988.
4. Kataoka, I. and Ishii, M., Mechanistic Modeling and Correlations for Pool-Entrainment Phenomenon, NUREG/CR-3304, ANL-83-37, Argonne National Laboratory, 1983.
5. Kataoka, I. and Ishii, M., "Mechanistic Modeling of Pool Entrainment Phenomenon," Int. J. Heat Mass Transfer, Vol. 27, No. 11, pp 1997-2014, 1984.
6. Blottner, F. G., Hydrodynamics and Heat Transfer Characteristics of Liquid Pools with Bubble Agitation, NUREG/CR-0944, SAND79-1132, Sandia National Laboratories, 1979.
7. Wilson, J. F., Grenda, R. J. and Patterson, J. F., "The Velocity of Rising Steam in a Bubbling Two-Phase Mixture," Transactions of the American Nuclear Society, Number 1, 1962 Annual Meeting, Boston, MA, June 1962.
8. Sterman, L. S., "The Generation of Experimental Data Concerning the Bubbling of Vapor Through Liquid," Soviet Technical Physics, Vol. 1, No. 7, pp 1479-1485, 1957.
9. Hughmark, G. A., "Holdup and Mass Transfer in Bubble Columns," Ind. Eng. Chem. Process Design and Develop., Vol. 6, pp 218-220, 1967.
10. Gonzales, F. G., "Liquid-Liquid Entrainment by Gas Injection in a Pool Configuration," Ph.D. Thesis, Nuclear Engineering and Engineering Physics, University of Wisconsin-Madison, 1987.

11. Clift, Grace and Weber, Bubbles Drops and Particles,
12. Renjun, Z., Xinzhen, J., Baozhang, L., Yong, Z., and Laiqi, Z., "Studies on Gas Holdup in a Bubble Column Operated at Elevated Temperatures," Ind. Eng. Chem. Res., Vol. 27, pp 1910-1916, 1988.
13. Project Information Sheet, Dense Alundum Castable Cements, CA331, CA332, CA334 and CA335. Norton Refractories Division, Norton Company, Worchester, MA.
14. Thermophysical Properties of Matter, the TPRC Data Series, Touloukian Y. S. and Ho, C. Y., Editors, IFI Plenum, 1975, Vol. 13, pp 1278-1171, New York, NY, 1975.
15. Ibid., Volume 12, pp 1166-1171.
16. Smithells, C. J., Metals Reference Book, Fourth Edition, Butterworth and Co. (Publishers) Ltd., London, 1967.
17. CRC Handbook of Chemistry and Physics, 59th Edition, 1978-1979, Chemical Rubber Company, Cleveland, OH, 1978.
18. Baron, P. A., "Calibration and Use of the Aerodynamic Particle Sizer (APS 3300)," Aerosol Science and Technology, Vol. 5, p 55-67, 1986.
19. Eckert, E. R. G., and Drake, R. M., Jr., Analysis of Heat and Mass Transfer, McGraw-Hill Book Company, New York, NY 1972.

DISTRIBUTION:

U. S. Nuclear Regulatory Commission (17)
Office of Nuclear Regulatory Research

Attn: B. Sheron
C. N. Kelber
N. Costanzi
G. Marino
F. Eltawila
R. W. Wright
T. Walker
R. O. Meyer
J. Mitchell
C. Tinkler (5)
P. Worthington
S. B. Burson
M. Cunningham

Washington, D.C. 20555

U. S. Nuclear Regulatory Commission (4)
Office of Nuclear Reactor Regulation

Attn: P. Easky
J. Rosenthal
B. Hardin
R. Barrett

Washington, D.C. 20555

U. S. Nuclear Regulatory Commission (6)
NRC/RES

Attn: E. Beckjord
T. Lee
W. Lyon
Z. Rosztoczy
C. Ryder
T. Speis

Washington, D.C. 20555

U. S. Department of Energy (2)
Albuquerque Operations Office

Attn: C. E. Garcia, Director
For: C. B. Quinn
R. L. Holton

P. O. Box 5400
Albuquerque, NM 87185

Electric Power Research Institute (4)

Attn: F. Rahn
R. Ritzman
W. Lowenstein
R. Sehgal

3412 Hillview Avenue
Palo Alto, CA 94303

Brookhaven National Laboratory (6)

Attn: R. A. Bari
T. Pratt
G. Greene
T. Ginsberg
M. Lee
N. Tutu

130 BNL
Upton, NY 11973

Professor R. Seale
Department of Nuclear Engineering
University of Arizona
Tucson, AZ 85721

Oak Ridge National Laboratory (2)

Attn: T. Kress
A. Wright
P. O. Box Y
Oak Ridge, TN 37830

Argonne National Laboratory (8)

Attn: J. Rest
C. Johnson
L. Baker, Jr.
D. Cho
B. Spencer
K. Leong
J. Fink
V. Novick

9700 S. Cass Avenue
Argonne, IL 60439

Cathy Anderson
Nuclear Safety Oversight Commission
1133 15th Street, NW
Room 307
Washington, D.C. 20005

Battelle Columbus Laboratory (4)

Attn: C. Alexander
P. Cybulskis
R. Denning
J. Gieseke

505 King Avenue
Columbus, OH 43201

J. E. Antill
Berkeley Nuclear Laboratory
Berkeley GL 139PB
Gloucestershire, England
UNITED KINGDOM

W. G. Cunliffe
Bldg. 396
British Nuclear Fuels, Ltd.
Springfield Works
Salwick, Preston
Lancashire, England
UNITED KINGDOM

Professor Agustin Alonso
E.T.S. Ingenieros Industriales
Jost Gutierrez Abascal, 2
28006 Madrid
SPAIN

Dr. Alfonso Perez
Departamento de Seguridad Nuclear
Junta de Energia Nuclear
Avenida Complutense, 22
Madrid - 3
SPAIN

R. Sherry
JAYCOR
P. O. Box 85154
San Diego, CA 92138

Los Alamos National Laboratories
Attn: M. Stevenson
P.O. Box 1663
Los Alamos, NM 87545

UCLA (2)
Nuclear Energy Laboratory
Attn: I. Catton
D. Okrent
405 Hilgaard Avenue
Los Angeles, CA 90024

University of Wisconsin
Nuclear Engineering Department
Attn: M. L. Corradini
1500 Johnson Drive
Madison, WI 53706

EG&G Idaho
Willow Creek Building, W-3
Attn: R. Hobbins
P. O. Box 1625
Idaho Falls, ID 83415

Battelle Pacific Northwest Laboratory
Attn: M. Freshley
P. O. Box 999
Richland, WA 99352

W. Stratton
2 Acoma Lane
Los Alamos, NM 87544

Gesellschaft fur Reaktorsicherheit (GRS)
Postfach 101650
Glockengrass 2
5000 Koeln 1
FEDERAL REPUBLIC of GERMANY

Kraftwerk Union
Attn: Dr. M. Peehs
Hammerbacher Strasse 1214
Postfach 3220
D-8520 Erlangen 2
FEDERAL REPUBLIC of GERMANY

UKAEA (8)
Attn: R. Potter 209/A32
A. Nicholas 102/A50
B. Bowsher 105A/A50
J. Mitchell 01/A50
B. Morris 216/A32
P. Smith 215/A32
S. Kinnersly 203/A32
D. Williams 210/A32
Winfrith, Dorchester
Dorset DT2 8DH
UNITED KINGDOM

Nucleare e della Protezione Sanitaria (DISP) (2)
Attn: Mr. Manilia
Mr. G. Petrangeli
Ente Nazionnle Energie Alternative (ENEA)
Viale Regina Margherita, 125
Casella Postale M. 2358
I-00100 Roma A. D.
ITALY

Dr. K. J. Brinkman
Reactor Centrum Nederland
1755 ZG Petten
THE NETHERLANDS

Dr. S. J. Niemczyk
1545 18th Street, NW
#112
Washington, D.C. 20036

Kernforschungszentrum Karlsruhe (2)
Attn: H. Alsmeyer
H. Rininsland
Postfach 3640
75 Karlsruhe
FEDERAL REPUBLIC of GERMANY

Mr. H. Bairiot, Chief
Department LWR Fuel
Belgonucleaire
Rue de Champde Mars. 25
B-1050 Brussels
BELGIUM

Japan Atomic Energy Research Institute
Attn: S. Saito
Tokai-Mura, Naka-Gun
Ibaraki-Ken 319-11
JAPAN

Wang Lu
TVA
400 Commerce, W9C157-CK
Knoxville, TN 37902

Peter Bieniarz
Risk Management Associates
2309 Dietz Farm Road, NW
Albuquerque, NM 87107

Dr. K. Soda
Fuel Reliability Laboratory
Department of Nuclear Fuel Safety
Japan Atomic Energy Research Institute
Tokai-Mura, Naka-Gun, Ibaraki-Ken
319-11
JAPAN

K. Sato, Director
Department of Reactor Safety Research
Japan Atomic Energy Research Institute
Tokai-Mura, Naka-Gun, Ibaraki-Ken
319-11
JAPAN

P. Fehrenback
Atomic Energy Canada, Ltd.
Chalk River, Ontario
CANADA KOJ IJO

UKAEA (2)
Attn: A. Taig
M. Haynes
Safety and Reliability Directorate
Wigshaw Lane
Culcheth
Warrington WA3 4NE
Cheshire
UNITED KINGDOM

J. R. Mathews
Aere Harwell
Didcot
Oxfordshire OX11 0RA
UNITED KINGDOM

UKAEA Culham Laboratory (3)
Attn: N. J. Brealey E5.152
B. D. Turland E5.157
F. Briscoe
Abingdon
Oxfordshire OX14 3DB
UNITED KINGDOM

H. J. Teague (3)
UKAEA
Safety and Reliability Directorate
Wigshaw Lane
Culcheth
Warrington, WA3 4NE
UNITED KINGDOM

M. Jankowski
IAEA
Division of Nuclear Reactor Safety
Wagranesrstrasse 5
P. O. Box 100
A/1400 Vienna
AUSTRIA

Statens Karnkraftinspektion (2)
Attn: L. Hammer
W. Frid
P. O. Box 27106
S-10252 Stockholm
SWEDEN

Studvik Energiteknik AB
Attn: K. Johansson
S-611 82 Nykoping
SWEDEN

Atomic Energy Canada Ltd. (2)
Attn: H. Rosinger
D. Wren
Pinawa, Manitoba
CANADA ROE 1LO

Korea Adv Energy Research Inst
Attn: H. R. Jun
P. O. Box 7
Daeduk-Danji
Choong-Nam
KOREA

Institute of Nuclear Energy Research
Attn: Sen-I Chang
P. O. Box 3
Lungtan
Taiwan 325
REPUBLIC OF CHINA

Juan Bagues
Consejo de Seguridad Nuclear
SOR Angela de la Cruz No 3
Madrid 28056
SPAIN

U. S. Department of Energy
Office of Nuclear Safety Coordination
Attn: R. W. Barber
Washington, D.C. 20545

Department of Energy
Scientific and Tech. Info. Center
P. O. Box 62
Oak Ridge, TN 37831

Power Authority State of New York
Attn: R. Deem
10 Columbus Circle
New York, NY 10019

M. Fontana
Director, IDCOR Program
ENERGEX
575 Oak Ridge Turnpike
Oak Ridge, TN 37830

Fauske and Associates, Inc. (2)
Attn: R. Henry
M. Plys
16W070 West 83rd Street
Burr Ridge, IL 60952

UKAEA
Reactor Development Division
Attn: T. Butland
Winfrith, Dorchester
Dorset DT2 9DH
England
UNITED KINGDOM

3141 S. A. Landenberger (5)
3151 W. I. Klein
6321 B. D. Zak
6400 D. J. McCloskey
6410 D. A. Dahlgren
6412 A. L. Camp
6415 R. M. Cranwell
6418 R. K. Cole
6420 W. B. Gauster
6422 D. A. Powers (5)
6422 M. D. Allen
6422 F. E. Arellano
6422 R. Blöse
6422 J. E. Brockmann (10)
6422 R. M. Elrick
6422 E. R. Copus
6422 D. A. Lucero
6422 D. Sweet
6422 M. Pilch
6423 K. O. Reil
6425 S. S. Dosanjh
6425 B. R. Bradley
6425 K. D. Bergeron
6429 F. Gelbard
6429 D. C. Williams
6454 G. L. Cano
6523 W. A. Von Rieseemann
8524 J. A. Wackerly

BIBLIOGRAPHIC DATA SHEET

(See instructions on the reverse)

1. REPORT NUMBER
(Assigned by NRC. Add Vol., Supp., Rev.,
and Addendum Numbers, if any.)

NUREG/CR-5433
SAND89-1951

2. TITLE AND SUBTITLE

Validation of Models of Gas Holdup in the CORCON Code

3. DATE REPORT PUBLISHED

MONTH: | YEAR:

December | 1989

4. FIN OR GRANT NUMBER

A1832

5. AUTHOR(S)

J. E. Brockmann, F. E. Arellano, D. A. Lucero

6. TYPE OF REPORT

Technical

7. PERIOD COVERED (Include Dates)

8. PERFORMING ORGANIZATION - NAME AND ADDRESS (If NRC, provide Division, Office or Region, U.S. Nuclear Regulatory Commission, and mailing address; if contractor, provide name and mailing address.)

Sandia National Laboratories
Albuquerque, NM 87185

9. SPONSORING ORGANIZATION - NAME AND ADDRESS (If NRC, type "Same as above"; if contractor, provide NRC Division, Office or Region, U.S. Nuclear Regulatory Commission, and mailing address.)

Division of Systems Research
Office of Nuclear Regulatory Research
U. S. Nuclear Regulatory Commission
Washington, D.C. 20555

10. SUPPLEMENTARY NOTES

11. ABSTRACT (200 words or less)

Gas holdup data for oleic acid at 291 K and for 1018 steel at 1823 K has been taken for nitrogen sparging gas. The liquid levels have been measured using a real time x-ray technique. The data have been compared to correlations from the literature to assess the appropriate correlations for use in calculating gas holdup for molten core debris in reactor accident calculations. A suitable correlation has been determined as well as coefficients for use in a drift flux model.

12. KEY WORDS/DESCRIPTORS (List words or phrases that will assist researchers in locating the report.)

Holdup
Gas Sparging
Level Swell
Melt-Concrete Interaction
CORCON

13. AVAILABILITY STATEMENT

Unlimited

14. SECURITY CLASSIFICATION

(This Page)

Unclassified

(This Report)

Unclassified

15. NUMBER OF PAGES

16. PRICE

UNITED STATES
NUCLEAR REGULATORY COMMISSION
WASHINGTON, D.C. 20555

OFFICIAL BUSINESS
PENALTY FOR PRIVATE USE, \$300

SPECIAL FOURTH CLASS RATE
POSTAGE & FEES PAID
USNRC
PERMIT No. G-67

120555139531 1 1A1R31R41R7
US NRC-OADM
DIV FOIA & PUBLICATIONS SVCS
TPS PDR-NUREG
P-223
WASHINGTON DC 20555